

Contribution from the Department of Chemistry, University of Chicago,  
Chicago, Illinois 60637

## Tricyclic Complexes, $[M(C_{14}H_{24}N_8O_2)L_2]X_n$ , Obtained from the Condensation of Formaldehyde with Octaaza Macrocyclic Complexes, $[M(C_{10}H_{20}N_8)]^{n+}$ : Synthesis, Studies, and X-Ray Structural Characterization

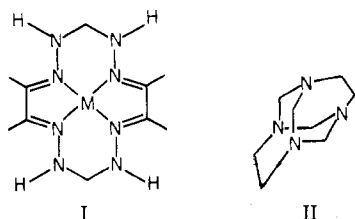
SHIE-MING PENG and VIRGIL L. GOEDKEN\*<sup>1</sup>

Received July 18, 1977

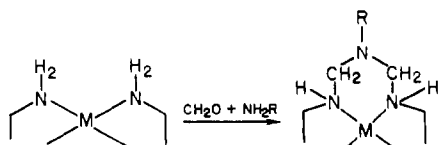
The octaazabis( $\alpha$ -diimine) macrocyclic complexes of the type  $[M(C_{10}H_{20}N_8)]^{n+}$  ( $M = Fe(II), Co(II), Co(III), Ni(II), Cu(II)$ ) react with formaldehyde giving tricyclic macroring tetradentate ligand complexes,  $[M(C_{14}H_{24}N_8O_2)]^{n+}$ . Formaldehyde attacks the secondary nitrogen centers forming a  $-CH_2-O-CH_2-$  linkage between the uncoordinated nitrogen atoms. Isomeric products in which the  $-CH_2-O-CH_2-$  linkages have formed on the same (syn) or opposite (anti) sides of the macrocyclic ligand plane have been identified. Crystal structures of two complexes,  $[Cu(C_{14}H_{24}N_8O_2)(H_2O)](ClO_4)_2$  and  $[Co(C_{14}H_{24}N_8O_2)(CH_3CN)_2](ClO_4)_3$  have been determined from three-dimensional x-ray crystal data. The structure of the  $[Co(C_{14}H_{24}N_8O_2)(H_2O)](ClO_4)_2$  complex was shown to be isomorphous with the Cu(II) analogue. Pertinent crystal data are the following:  $[Cu(C_{14}H_{24}N_8O_2)(H_2O)](ClO_4)_2$ , space group  $C_{2h}^6-C2/c$ ,  $a = 16.697(2) \text{ \AA}$ ,  $b = 7.8196(9) \text{ \AA}$ ,  $c = 18.904(2) \text{ \AA}$ ,  $\beta = 100.42^\circ$ ,  $\rho_{\text{calcd}} = 1.687 \text{ g/cm}^3$ ,  $\rho_{\text{exptl}} = 1.68(3) \text{ g/cm}^3$  for  $Z = 4$ ;  $[Co(C_{14}H_{24}N_8O_2)(CH_3CN)_2](ClO_4)_3$ , space group =  $D_{2h}^{15}-Pbca$ ,  $a = 17.346(4) \text{ \AA}$ ,  $b = 21.001(5) \text{ \AA}$ ,  $c = 17.145(5) \text{ \AA}$ ,  $\rho_{\text{calcd}} = 1.650 \text{ g/cm}^3$ ,  $\rho_{\text{exptl}} = 1.63(3) \text{ g/cm}^3$  for  $Z = 8$ . The  $-CH_2-O-CH_2-$  linkages in each structure are on the same side of the ligand. The  $H_2O$  of the Cu(II) complex is coordinated to the least encumbered side of the molecule and symmetrically hydrogen bonded to the two perchlorate anions. The average Cu-N bond distance is  $1.936(8) \text{ \AA}$ ; the Cu-O distance is  $2.262(6) \text{ \AA}$ . High thermal motions and apparent disorder of the  $ClO_4^-$  oxygen atoms precluded accurate refinement of the Co(III) structure. The average Co-N (macrocycle) distance is  $1.90(1) \text{ \AA}$ ; the average Co-N( $CH_3CN$ ) distance is  $1.89(1) \text{ \AA}$ . In neither complex do the oxygen atoms of the six-membered ring interact significantly with the axial coordination sites.

### Introduction

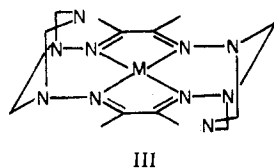
Properly designed macrocyclic ligands provide a stable framework on which to build peripheral groups which may be chosen to interact with vacant coordination sites or selectively block access to axial sites by certain or all substrates.<sup>2-4</sup> The octaaza macrocyclic complexes, I, obtained by the metal



template condensation of 2,3-butanedione dihydrazone with aldehydes<sup>5</sup> have uncoordinated secondary nitrogen atoms which are capable of undergoing further reactions with aldehydes. The nature of these condensations was expected to be analogous to those of formaldehyde with ammonia which yield hexamethylenetetramine and to those of formaldehyde with ethylenediamine to yield the lesser known product, II.<sup>6</sup> Amine ligands have also been shown to undergo condensation reactions with formaldehyde and other amines to yield new polydentate ligands as indicated below.<sup>7</sup>

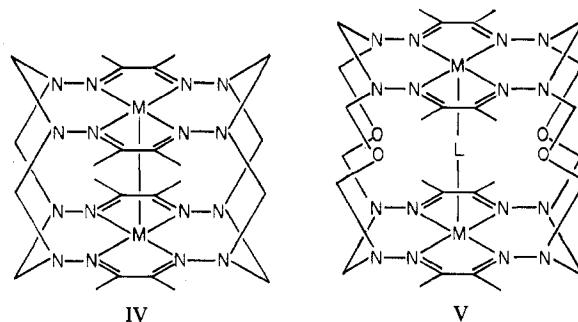


It was therefore expected that I might undergo further condensation reactions with formaldehyde and ammonia to yield a tricyclic macroring ligand III in which two triaza-



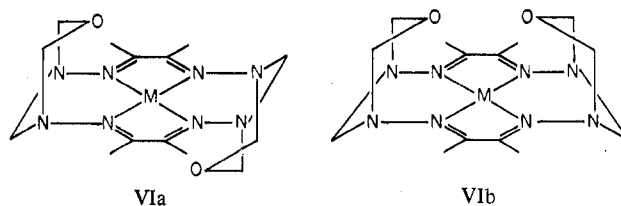
cyclohexane rings were fused to the original 14-membered

macrocyclic ring. Other possibilities envisaged were the formation of cofacial binuclear dimers such as IV, V, or



polymeric species. Dreiding models indicate that structures such as IV might be possible if a metal-metal bond formed; the formation and stabilization of structures such as V would be assisted by an additional bridging ligand between the two metals.

The products obtained in all cases were of type VI which



formally result from the condensation of four molecules of formaldehyde with the macrocyclic complexes of type I. This paper is an account of the synthesis and characterization of these complexes, including three-dimensional x-ray structure determinations of two complexes,  $[Cu(C_{14}H_{24}N_8O_2)(H_2O)](ClO_4)_2$  and  $[Co(C_{14}H_{24}N_8O_2)(CH_3CN)_2](ClO_4)_3$ , which contain the isomeric form of the ligand depicted in VIb.

### Experimental Section

All solvents and chemicals used in the experiments were obtained commercially and were of reagent grade; they were used without further purification except for drying with 4A molecular sieves.

All infrared spectra were recorded on a Beckman IR-10 infrared spectrophotometer in the range of  $4000-250 \text{ cm}^{-1}$ . Samples were

Table I. Crystal Data for the Tricyclic Complexes

	$[Co(C_{14}H_{24}N_8O_2)(CH_3CN)_2](ClO_4)_3$	$[Cu(C_{14}H_{24}N_8O_2)(H_2O)](ClO_4)_2$	$[Co(C_{14}H_{24}N_8O_2)(H_2O)](ClO_4)_2$
Formula wt	775.79	616.85	612.24
Space group	<i>Pbca</i>	<i>C2/c</i>	<i>C2/c</i>
<i>a</i> , Å	17.346 (4)	16.6971 (15)	16.714 (6)
<i>b</i> , Å	21.001 (5)	7.8196 (9)	8.111 (3)
<i>c</i> , Å	17.145 (5)	18.9040 (18)	18.304 (6)
$\alpha$ , deg	90.0 (0)	90.0 (0)	90.0 (0)
$\beta$ , deg	90.0 (0)	100.42 (1)	98.78 (2)
$\gamma$ , deg	90.0 (0)	90.0 (0)	90.0 (0)
No. of reflections used to determine cell constants	12	25	12
$2\theta$	$20 \leq 2\theta \leq 30^\circ$	$30 \leq 2\theta \leq 35^\circ$	$20 \leq 2\theta \leq 30^\circ$
$d_{\text{calcd}}$ , g/cm <sup>3</sup>	1.650	1.687	1.687
$d_{\text{exptl}}$ , g/cm <sup>3</sup>	1.63 (3)	1.68 (3)	1.68 (3)

prepared as Nujol or hexachlorobutadiene mulls and the spectra were calibrated with the 2951.5- and 1601.8-cm<sup>-1</sup> absorptions of polystyrene film. A Beckman RC 16B2 conductivity bridge was used for all conductivity measurements. Ultraviolet and visible spectra within the range 10 000–2000 Å were obtained using a Cary Model 14 recording spectrophotometer. Nuclear magnetic resonance spectra were recorded on either Varian A-60 A or Bruker 270-MHz spectrometers.

Elemental analyses were performed commercially by Galbraith Laboratories, Inc., Knoxville, Tenn., or Chemalytic, Inc., Tempe, Ariz.

Magnetic susceptibilities of the complexes were measured on a Faraday balance using HgCo(NCS)<sub>4</sub> as a calibrant. Molar susceptibilities were corrected for diamagnetism of the ligands with Pascal's constants.

**Warning!** Some of the compounds containing perchlorate anions must be regarded as extremely hazardous and potentially explosive. Since the possibility of unprovoked detonation exists, only minimal quantities should be prepared and we do not recommend long term storage (greater than 1 month).

**Syntheses of Tricyclic Complexes.** The macrocyclic precursor complexes  $[M(C_{10}H_{20}N_8)X_2]^{n+}$  were prepared as previously described.<sup>5</sup>

$[Ni(C_{14}H_{24}N_8O_2)](ClO_4)_2$ . A solution was prepared by dissolving 2.04 g (4 mmol) of the cyclic complex  $[Ni(C_{10}H_{20}N_8)](ClO_4)_2$  in 25 mL of acetonitrile. Then 1.44 g of an aqueous solution of 37% formaldehyde (16 mmol) was added, followed by 0.5 mL of concentrated perchloric acid catalyst. The orange product started precipitating within 1 min. After 0.5 h the product was filtered, washed with acetonitrile, and air-dried. Yield is about 90%.

Anal. Calcd: C, 28.29; H, 4.04; N, 18.87. Found: C, 28.06; H, 4.20; N, 17.86.

$[Fe(C_{14}H_{24}N_8O_2)(CH_3CN)_2](ClO_4)_2$ . The procedure was similar to that described above, but since the product is soluble in acetonitrile, diethyl ether was added drop by drop to precipitate the pink-red product. Yield is 80%.

Anal. Calcd: C, 32.09; H, 4.46; N, 20.81. Found: C, 30.35; H, 4.19; N, 19.01.

$[Fe(C_{14}H_{24}N_8O_2)(CNCH_3)_2](ClO_4)_2$ . One gram of the bis(acetonitrile) complex was dissolved in acetonitrile and 0.25 mL of methyl isocyanide was added at room temperature. Diethyl ether was added dropwise to facilitate precipitation of the complex and the solution was allowed to stand in a refrigerator for 2 h. The precipitate was filtered, washed with ethanol, and dried in vacuo. Yield is about 80%.

Anal. Calcd: C, 32.09; H, 4.46; N, 20.81. Found: C, 30.22; H, 4.60; N, 20.77.

$[Fe(C_{14}H_{24}N_8O_2)(NCS)_2]$ .  $[Fe(C_{14}H_{22}N_8O_2)(CH_3CN)_2](ClO_4)_2$  (1.35 g) was dissolved in 30 mL of acetonitrile and NaNCS solution, 0.5 g of NaNCS in 20 mL of acetonitrile, was added. The blue product precipitated immediately. The product was filtered and washed with acetonitrile and air-dried. The yield was virtually quantitative.

Anal. Calcd: C, 37.81; H, 4.73; N, 27.56; S, 12.59. Found: C, 37.66; H, 4.81; N, 27.38; S, 12.66.

$[Fe(C_{14}H_{24}N_8O_2)(C_3H_5N)_2](ClO_4)_2$ . To a solution of 1.35 g of  $[Fe(C_{14}H_{22}N_8O_2)(CH_3CN)_2](ClO_4)_2$  in 20 mL of acetonitrile, a large excess of pyridine, 5 mL, was added. The color of the solution changed immediately from pink-red to blue. Diethyl ether was added drop by drop to precipitate the product. The product was filtered and washed by methanol and dried in air. Yield is 90%.

Anal. Calcd: C, 37.66; H, 4.61; N, 19.32. Found: C, 38.45; H, 4.54; N, 18.69.

$[Cu(C_{14}H_{24}N_8O_2)(H_2O)](ClO_4)_2$ . To a solution of 1.8 g of  $[Cu(C_{10}H_{20}N_8)Cl(H_2O)](ClO_4)$  in 25 mL of acetonitrile, 1.44 g of 37% aqueous solution of formaldehyde was added, followed by 1 mL of concentrated perchloric acid. The red crystalline product formed after approximately 0.5 h. The product was filtered, washed with 1:1 acetonitrile-diethyl ether mixture and air-dried. Yield is about 60%.

Anal. Calcd: C, 27.25; H, 4.21; N, 18.16; Cl, 11.52. Found: C, 26.62; H, 4.10; N, 17.99; Cl, 11.87.

$[Co(C_{14}H_{24}N_8O_2)(H_2O)](ClO_4)_2$ . The procedure was the same as for the Cu(II) complex. The starting material was  $[Co(C_{10}H_{14}N_8)](ClO_4)_2$  and the reaction was carried out under N<sub>2</sub>. Yield is about 80%.

Anal. Calcd: C, 27.45; H, 4.25; N, 18.30. Found: C, 26.67; H, 4.30; N, 17.85.

$[Co(C_{14}H_{24}N_8O_2)(CH_3CN)_2](ClO_4)_2$ . A solution of the aquo complex described above was prepared by dissolving 1 g in 15 mL of acetonitrile. Triethyl orthoformate, 0.5 mL, was added and then the solution was warmed at 40 °C for 1 h to dehydrate the solution. Precipitation of the complex was facilitated by the dropwise addition of diethyl ether until the solution became turbid. The solution was then placed in a refrigerator for several hours to ensure more complete precipitation of the product. The orange crystalline material was filtered, washed with anhydrous ethanol and dried in vacuo.

Anal. Calcd: C, 31.94; H, 4.44; N, 20.70; Cl, 10.48. Found: C, 31.80; H, 4.54; N, 20.42; Cl, 10.53.

$[Co(C_{14}H_{24}N_8O_2)(CH_3CN)_2](ClO_4)_3$ . The procedure was the same as above, but the solution was bubbled with molecular oxygen for 0.5 h. The oxidation of Co(II) to Co(III) is slow in this case.

Anal. Calcd: C, 27.83; H, 3.87; N, 18.04; Cl, 13.72. Found: C, 27.38; H, 3.93; N, 17.77; Cl, 13.16.

### Details of the X-Ray Structure Determinations

**Crystal Examination and Data Collection.** X-ray precession photographs of  $[Cu(C_{14}H_{24}N_8O_2)(H_2O)](ClO_4)_2$  exhibited monoclinic symmetry with systematic absences consistent with either *C2/c-C2h*<sup>6</sup> or *Cc-C2h*<sup>4</sup> space groups.<sup>8</sup> Subsequent satisfactory refinement assuming the centrosymmetric space group confirmed *C2/c* as the correct space group. Lattice constants and their estimated standard deviations, together with the other pertinent crystal data, are given in Table I. The lattice parameters for the isomorphous Co(II) compound are listed in the table for comparison.

Precession photographs of  $[Co(C_{14}H_{24}N_8O_2)(CH_3CN)_2](ClO_4)_3$  indicated an orthorhombic cell; the systematic absences indicated *Pbca-D2h*<sup>15,9</sup> as the unique space group. The lattice parameters and other important crystal data are given in Table I.

The details of the data collection for the Cu(II) and Co(III) complexes are presented in Table II.<sup>10</sup> The data were reduced in the conventional manner with corrections for Lorentz and polarization effects. Estimated standard deviations of the reflection intensities and derived *F*<sup>2</sup>'s based primarily on counting statistics were calculated using the following equation:

$$\sigma(I) = [S + \frac{T_s^2(B_1B_2)}{T_B^2(B_1 + B_2)} + (pS)^2]^{1/2} \quad (1)$$

*S*, *B*<sub>1</sub>, and *B*<sub>2</sub> are the accumulated counts for the scan and the two backgrounds, *T*<sub>s</sub> and *T*<sub>B</sub> are the scan and individual background

Table II. Data Collection Details for Tricyclic Complexes

	[Co(C <sub>14</sub> H <sub>24</sub> N <sub>8</sub> O <sub>2</sub> )(CH <sub>3</sub> CN) <sub>2</sub> ](ClO <sub>4</sub> ) <sub>3</sub>	[Cu(C <sub>14</sub> H <sub>24</sub> N <sub>8</sub> O <sub>2</sub> )(H <sub>2</sub> O)](ClO <sub>4</sub> ) <sub>2</sub>
Diffractometer	Picker-FACS-1	Picker-FACS-1
Monochromator (Bragg angle)	Graphite (6.093)	Graphite (6.093)
λ (Kα), Å	0.71069 (Mo)	0.71069 (Mo)
Takeoff angle, deg	3.0	3.0
Method	θ-2θ	θ-2θ
Scan speed, deg/min	1	2
Scan width, deg (2θ = 0°)	2	2.3
Background time, s	2 × 20	2 × 20
Standards	3	3
Av max deviation of standards from mean, %	2	2
2θ limits of data	0 < 2θ < 55°	0 < 2θ < 55°
No. of data collected	7165 (unique)	2793 (unique)
No. of data used in final refinement	4231 (F ≥ 2σ(F))	2129 (F ≥ 3σ(F))
Absorption coefficients, cm <sup>-1</sup>	9.12	12.28
Crystal dimension, mm	0.09 × 0.11 × 0.22	0.10 × 0.40 × 0.20

counting times, and  $p$  is a factor,<sup>11</sup> here taken to be 0.02, to account for machine fluctuations and other factors which would be expected to cause variations proportional to the reflected intensity. The  $F^2$ 's and  $F$ 's were calculated in the usual way from the intensities and the ( $F$ )'s were calculated using the approximation

$$\sigma(F) = \sigma(I)/2F(Lp)^{1/2}$$

A total of 2129 independent reflections having  $F^2 \geq 3\sigma(F)$  were used in the refinement of the Cu(II) complex and 4231 data with  $F^2 \geq 2\sigma(F)$  for the Co(II) complex.

The effects of absorption ( $\mu = 12.28$  and  $9.12$  for the Cu(II) and Co(III) complexes) were judged to be minimal and were not compensated for.

**Structural Solution and Refinement of the Structures.** Both structures were solved by standard heavy-atom methods and refined by full-matrix least-squares techniques.<sup>12</sup> Scattering factors of neutral atoms were taken from standard sources.<sup>13</sup> Corrections for anomalous

dispersion were applied to the copper, cobalt, and chlorine atoms from the values of  $\Delta f'$  and  $\Delta f''$  tabulated by Cromer.<sup>14</sup> The details of the solution and refinement of the structures are summarized in Table III.

[Co(C<sub>14</sub>H<sub>24</sub>N<sub>8</sub>O<sub>2</sub>)(CH<sub>3</sub>CN)<sub>2</sub>](ClO<sub>4</sub>)<sub>3</sub>. The position of the cobalt atom was determined from a Patterson map. Successive Fourier maps based upon the phases generated from the coordinates of the cobalt atom revealed the location of the remaining nonhydrogen atoms. Refinement of the positional parameters and isotropic thermal parameters using the 1588 most intense data within the sphere  $2\theta \leq 40^\circ$  yielded a conventional  $R$  factor of 11.6%. Two cycles of full-matrix least-squares refinement the positional and isotropic thermal parameters using an expanded data set of the 2244 most intense data yielded  $R_1 = 14.0\%$  and  $R_2 = 13.8\%$ . A difference Fourier map calculated at this time revealed most of the hydrogen atom positions; enough methyl group hydrogen atoms were located to calculate the positions of those unobserved. The positions of all hydrogen atoms were then recalculated, using a least-squares fit and assuming idealized standard geometry ( $sp^3$  hybridization) and C-H distances of  $0.95 \text{ \AA}$ .<sup>15</sup> The contributions of the hydrogen atoms were included as fixed quantities in the subsequent cycles of least-squares refinement. The final cycles of refinement utilized 4231 data with  $F^2 \geq 2\sigma(F)$  within the sphere  $0 \leq 2\theta \leq 55^\circ$  and varied the positional parameters for all atoms, the anisotropic thermal parameters for the Co and ClO<sub>4</sub><sup>-</sup> atoms, and the isotropic thermal parameters for the remaining nonhydrogen atoms. At convergence,  $R_1 = 14.8\%$  and  $R_2 = 14.1\%$ .

The final difference Fourier map had residual peaks of  $1.6 \text{ e/\AA}^3$  between the oxygen atoms of the ClO<sub>4</sub><sup>-</sup> anions with a noise level of less than  $0.4 \text{ e/\AA}^3$ . Despite the high "R factor" the general features of the macrocyclic complex appear to be reasonably resolved. The estimated standard deviations of the C-C and C-N bond lengths are in the range of  $0.01\text{--}0.02 \text{ \AA}$  and those of Co-N are  $0.01 \text{ \AA}$ . Equally important, the chemically equivalent bond lengths do not differ significantly from one another and the bond distances fall within accepted ranges. The one exception is the C(3)=N(5)(imine) bond length of  $1.25 \text{ \AA}$  which is  $0.04 \text{ \AA}$  shorter than the average of the three other C=N bond lengths.

The high  $R$  factor has its origin in the distressingly high degrees of thermal motions associated with the ClO<sub>4</sub><sup>-</sup> anions. This, combined with the fact that the three ClO<sub>4</sub><sup>-</sup> anions comprise nearly 40% of the compound's molecular weight, contributed to the very rapid fall-off of intensities with increasing  $2\theta$  values. "R" factors were calculated

Table III. Summary of Structure Determinations for Tricyclic Complexes

	[Co(C <sub>14</sub> H <sub>24</sub> N <sub>8</sub> O <sub>2</sub> )(CH <sub>3</sub> CN) <sub>2</sub> ](ClO <sub>4</sub> ) <sub>3</sub>	[Cu(C <sub>14</sub> H <sub>24</sub> N <sub>8</sub> O <sub>2</sub> )(H <sub>2</sub> O)](ClO <sub>4</sub> ) <sub>2</sub>
Method	Heavy atom Patterson technique	Heavy atom Patterson technique
Heavy atom position from Patterson	General position $x = 0.231$ $y = 0.115$ $z = 0.000$	Special position $x = 0.000$ $y = 0.094$ $z = 0.250$
Problems in refinement	High thermal motion and/or disorder of perchlorate	High thermal motion and/or disorder of perchlorate
No. of least-squares cycles used in refinement	6	6
Model for final cycle of refinement	Positional and anisotropic thermal parameters of Co and ClO <sub>4</sub> atoms varied. Positional and isotropic thermal parameters of remaining nonhydrogen atoms varied. Hydrogen atoms included as fixed contributions	Positional and anisotropic thermal parameters of all nonhydrogen atoms were varied. Hydrogen atoms were included as fixed contributions
Final $R_1$ <sup>a</sup>	14.9	7.2
$R_2$	14.1	5.9
Standard error of an observation of unit weight, $[\sum w( F_o  -  F_c )^2 / (NO - NV)]^{1/2}$	3.007	3.450
Highest peak in final difference Fourier	$1.6 \text{ e/\AA}^3$ around oxygen positions of ClO <sub>4</sub>	$0.8 \text{ e/\AA}^3$ around oxygen atoms of ClO <sub>4</sub>
Noise level of final difference Fourier	Less than $0.4 \text{ e/\AA}^3$	Less than $0.25 \text{ e/\AA}^3$
Ratio of observations to variable	16.2:1	13:1

<sup>a</sup>  $R_1 = \sum [||F_c| - |F_o||] / \sum |F_o|$ ,  $R_2 = \{\sum w[|F_c| - |F_o|]^2 / \sum w|F_o|^2\}^{1/2}$ .

Table IV. Final Positional and Thermal<sup>a</sup> Parameters of Nonhydrogen Atoms of  $[Co(C_{14}H_{24}N_8O_2)(CH_3CN)_2](ClO_4)_3$ 

Atom	x	y	z	$B_{11}$	$B_{22}$	$B_{33}$	$B_{12}$	$B_{13}$	$B_{23}$
Co	0.23185 (9)	0.11221 (8)	0.00694 (9)	17.9 (5)	17.5 (4)	18.2 (5)	2.5 (4)	-0.6 (4)	1.6 (4)
Cl1	0.1717 (3)	0.1234 (3)	0.4711 (4)	35 (2)	26 (1)	108 (4)	-2 (1)	-12 (2)	5 (2)
O1	0.2031 (9)	0.1775 (7)	0.4528 (11)	84 (9)	37 (5)	124 (11)	-12 (5)	-37 (8)	21 (6)
O2	0.1654 (18)	0.0364 (12)	0.4069 (15)	373 (24)	76 (10)	157 (15)	-78 (13)	-118 (16)	5 (10)
O3	0.1055 (13)	0.1352 (12)	0.5021 (17)	87 (11)	103 (10)	408 (22)	66 (9)	116 (14)	119 (13)
O4	0.2121 (9)	0.0847 (7)	0.5249 (10)	58 (8)	36 (4)	109 (10)	6 (5)	1 (7)	17 (5)
Cl2	0.4214 (2)	0.1722 (2)	0.2247 (2)	32 (1)	24 (1)	45 (2)	-5 (1)	-13 (1)	5 (1)
O5	0.4626 (7)	0.2284 (5)	0.2375 (8)	52 (5)	27 (3)	58 (6)	-13 (3)	-6 (5)	1 (4)
O6	0.4202 (11)	0.1619 (7)	0.1427 (9)	97 (9)	46 (5)	49 (7)	10 (6)	-19 (7)	-7 (5)
O7	0.4552 (9)	0.1196 (7)	0.2602 (9)	79 (8)	37 (4)	82 (8)	2 (5)	-33 (7)	21 (5)
O8	0.3460 (9)	0.1796 (8)	0.2496 (12)	53 (7)	55 (6)	126 (11)	-11 (5)	29 (8)	4 (7)
Cl3	0.4942 (3)	0.4289 (2)	0.1799 (3)	60 (2)	21 (1)	50 (2)	-5 (1)	17 (2)	-5 (1)
O9	0.4846 (11)	0.4820 (6)	0.2256 (9)	138 (12)	27 (3)	70 (9)	20 (6)	-10 (9)	-16 (4)
O10	0.4649 (13)	0.3779 (9)	0.2088 (13)	186 (15)	53 (6)	142 (14)	-66 (8)	103 (12)	-25 (8)
O11	0.5725 (13)	0.4154 (11)	0.1778 (14)	88 (11)	106 (10)	163 (15)	27 (9)	17 (11)	-36 (10)
O12	0.4801 (17)	0.4374 (10)	0.1021 (12)	300 (22)	65 (9)	65 (11)	21 (11)	-51 (12)	-13 (8)

Atom	x	y	z	$B, \text{Å}^2$	Atom	x	y	z	$B, \text{Å}^2$
O13	0.1613 (6)	0.1967 (5)	0.1675 (6)	4.8 (2)	C4	0.3378 (10)	0.0730 (8)	-0.1304 (11)	5.4 (4)
O14	0.3955 (7)	0.1883 (6)	-0.0686 (7)	5.3 (2)	C5	0.1789 (9)	0.1801 (7)	-0.1140 (9)	3.9 (3)
N1	0.1336 (6)	0.1516 (5)	0.0073 (6)	2.8 (3)	C6	0.1164 (8)	0.1839 (6)	-0.0547 (8)	3.5 (2)
N2	0.0825 (6)	0.1588 (5)	0.0706 (6)	3.2 (2)	C7	0.0925 (10)	0.2017 (8)	0.1240 (10)	5.2 (4)
N3	0.1620 (7)	0.0836 (5)	0.1588 (7)	3.6 (2)	C8	0.1669 (9)	0.1400 (8)	0.2088 (9)	4.5 (3)
N4	0.2276 (6)	0.0791 (5)	0.1090 (5)	2.6 (2)	C9	0.4318 (10)	0.1298 (9)	-0.0527 (10)	5.4 (4)
N5	0.3133 (6)	0.0742 (5)	0.0094 (6)	3.1 (2)	C10	0.3550 (13)	0.1863 (10)	-0.1372 (13)	7.1 (5)
N6	0.3823 (7)	0.0760 (6)	-0.0552 (7)	3.9 (2)	C11	0.2951 (8)	0.2352 (7)	0.0703 (8)	3.3 (2)
N7	0.2980 (8)	0.1368 (6)	-0.1466 (7)	4.4 (3)	C12	0.1584 (8)	-0.0093 (7)	-0.0505 (8)	3.4 (3)
N8	0.2376 (7)	0.1476 (5)	-0.0952 (6)	3.3 (2)	C13	0.2976 (10)	0.0153 (8)	0.2073 (10)	4.9 (3)
N9	0.2736 (6)	0.1890 (5)	0.0448 (6)	3.0 (2)	C14	0.4267 (10)	0.0173 (8)	0.0878 (10)	4.8 (3)
N10	0.1875 (6)	0.0357 (5)	-0.0321 (6)	2.7 (2)	C15	0.1693 (11)	0.2147 (9)	-0.1912 (12)	6.2 (4)
C1	0.0921 (8)	0.0873 (7)	0.1110 (8)	3.6 (3)	C16	0.0437 (9)	0.2223 (8)	-0.0660 (9)	4.7 (3)
C2	0.2883 (7)	0.0490 (6)	0.1325 (7)	2.9 (2)	C17	0.3206 (11)	0.2942 (9)	0.1036 (11)	6.1 (4)
C3	0.3508 (8)	0.0474 (6)	0.0716 (8)	3.0 (2)	C18	0.1198 (11)	-0.0678 (9)	-0.0714 (11)	5.7 (4)

<sup>a</sup> The form of anisotropic thermal parameter is  $\exp[-(B_{11}h^2 + B_{22}k^2 + B_{33}l^2 + 2B_{12}hk + 2B_{13}hl + 2B_{23}kl) \times 10^{-4}]$ .

Table V. Positional and Anisotropic Thermal<sup>a</sup> Parameters of Nonhydrogen Atoms for  $[Cu(C_{14}H_{24}N_8O_2)(H_2O)](ClO_4)_2$ 

Atom	x	y	z	$\beta_{11}$	$\beta_{22}$	$\beta_{33}$	$\beta_{12}$	$\beta_{13}$	$\beta_{23}$
Cu	0.0 (0)	0.0836 (1)	0.2500 (0)	35.8 (4)	172 (2)	19.7 (3)	0 (0)	-6.9 (3)	0 (0)
C1	0.3662 (1)	0.1325 (2)	0.0915 (1)	50.9 (8)	155 (3)	25.9 (5)	-1 (1)	6.4 (5)	-1 (1)
O1	0.3035 (4)	0.0553 (7)	0.0476 (3)	150 (4)	329 (15)	78 (3)	-92 (7)	-58 (3)	18 (6)
O2	0.3478 (5)	0.2847 (9)	0.1079 (6)	164 (6)	261 (15)	235 (8)	53 (8)	-38 (6)	-161 (9)
O3	0.3886 (5)	0.0400 (10)	0.1524 (4)	208 (7)	632 (24)	65 (3)	-156 (10)	-51 (4)	106 (7)
O4	0.4296 (5)	0.1492 (17)	0.0640 (4)	108 (5)	1619 (63)	103 (5)	-44 (15)	61 (4)	20 (13)
O5	0.0 (0)	-0.2056 (8)	0.2500 (0)	132 (6)	151 (13)	69 (3)	0 (0)	-60 (4)	0 (0)
O6	0.1223 (2)	0.3861 (5)	0.1776 (2)	46 (2)	258 (9)	28 (2)	-11 (4)	1 (1)	10 (3)
N1	-0.0004 (3)	0.1170 (5)	0.3516 (2)	33 (2)	168 (9)	20 (1)	-6 (3)	-1 (1)	6 (3)
N2	0.1153 (2)	0.1140 (5)	0.2826 (2)	34 (2)	154 (9)	21 (1)	8 (3)	-3 (1)	0 (3)
N3	0.1721 (3)	0.1229 (6)	0.2353 (2)	33 (2)	236 (11)	26 (2)	18 (4)	-1 (2)	-10 (3)
N4	0.0725 (3)	0.1251 (6)	0.1186 (2)	39 (2)	234 (11)	20 (2)	25 (4)	1 (1)	-14 (3)
C1	0.0699 (3)	0.1370 (6)	0.3913 (3)	40 (2)	101 (10)	17 (2)	-11 (4)	-4 (2)	7 (3)
C2	0.1389 (3)	0.1358 (6)	0.3503 (3)	31 (2)	100 (10)	22 (2)	5 (4)	-3 (1)	3 (3)
C3	0.1378 (4)	0.0337 (8)	0.1671 (3)	40 (3)	266 (14)	31 (2)	39 (5)	2 (2)	-31 (5)
C4	0.1900 (4)	0.3017 (9)	0.2193 (3)	41 (3)	303 (15)	32 (3)	-15 (6)	3 (2)	-1 (5)
C5	0.0978 (4)	0.3019 (8)	0.1107 (3)	46 (3)	321 (15)	22 (2)	6 (5)	4 (2)	11 (5)
C6	0.0845 (3)	0.1585 (7)	0.4706 (3)	55 (3)	222 (13)	19 (2)	-24 (5)	-6 (2)	10 (4)
C7	0.2240 (3)	0.1561 (7)	0.3878 (3)	35 (3)	185 (12)	27 (2)	4 (4)	-10 (2)	-7 (4)

<sup>a</sup> The thermal parameters are of the form  $\exp[-(\beta_{11}h^2 + \beta_{22}k^2 + \beta_{33}l^2 + 2\beta_{12}hk + 2\beta_{13}hl + 2\beta_{23}kl) \times 10^{-4}]$ .

in shells using increments of  $\theta = 5^\circ$  and also as a function of the magnitudes of the structure factors. In general, the agreement between observed and calculated structure factors was good for the lower angle and high intensity data but the agreement became progressively poorer as the data approached the  $2\sigma(F)$  cutoff limit. The final positional and thermal parameters are listed in Table IV.

$[Cu(C_{14}H_{24}N_8O_2)(H_2O)](ClO_4)_2$ . The coordinates of the copper and chlorine atoms were located from a Patterson synthesis. A Fourier map based on the phases obtained from the heavy atoms revealed all the nonhydrogen atom positions. Least-squares refinement of the scale factor, the positional and isotropic thermal parameters for the macrocyclic ligand atoms, and anisotropic thermal parameters of the copper atoms and those of the perchlorate anion converged to  $R_1 = 7.7\%$  and  $R_2 = 8.4\%$  using the 1155 most intense data. A difference Fourier revealed all the hydrogen atoms; their positions were re-

calculated assuming idealized geometry and C-H distances of 0.95 Å. All hydrogen atoms were assigned isotropic  $B$  values of 5 and included as fixed contributions in the last two cycles of the least-squares refinement. In the final cycles of refinement, the positional and anisotropic thermal parameters for all nonhydrogen atoms were varied. At convergence,  $R_1 = 7.2\%$  and  $R_2 = 5.9\%$  for 2129 data having  $F^2 \geq 3\sigma(F)$ . The final difference Fourier had a noise level of approximately  $0.25 \text{ e}/\text{Å}^3$  with the highest peak of  $0.8 \text{ e}/\text{Å}^3$  located in the vicinity of the oxygen atoms of the perchlorate ion. The final positional and thermal parameters for the copper complex are listed in Table V.

## Results and Discussion

The acid-catalyzed reaction of macrocyclic complexes, I, with aqueous formaldehyde yields tricyclic species of type VI.

Table VI.  $^1\text{H}$  NMR Data of Tricyclic Complexes

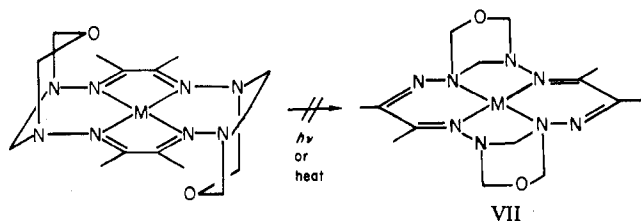
Compd	Solvent	Chemical shift <sup>b</sup>
$[\text{Fe}(\text{C}_{14}\text{H}_{24}\text{N}_8\text{O}_2)(\text{CH}_3\text{CN})_2](\text{ClO}_4)_2$	$\text{D}_2\text{O}/\text{CD}_3\text{CN}$ mixture	$\text{NC-CH}_3^a$ 1.97 (6, s), $-\text{CH}_3$ 2.86 (12, s), $-\text{CH}_2$ 4.6-5.8 (12, m)
<i>syn</i> - $[\text{Fe}(\text{C}_{14}\text{H}_{24}\text{N}_8\text{O}_2)(\text{CNCH}_3)_2](\text{ClO}_4)_2$	$\text{CD}_3\text{CN}$	$\text{CNCH}_3$ 3.26 (3), 3.05 (3), $-\text{CH}_3$ 2.57 (12, s), $-\text{CH}_2$ 4.5-5.9 (12, m)
<i>anti</i> - $[\text{Fe}(\text{C}_{14}\text{H}_{24}\text{N}_8\text{O}_2)(\text{CNCH}_3)_2](\text{ClO}_4)_2$	$\text{CD}_3\text{CN}$	$\text{CN-CH}_3$ 3.15 (6), $-\text{CH}_3$ , 2.57 (12, s), $-\text{CH}_2$ 4.5-6.0 (12, m)
<i>syn</i> - $[\text{Co}(\text{C}_{14}\text{H}_{24}\text{N}_8\text{O}_2)(\text{CH}_3\text{CN})_2](\text{ClO}_4)_3$	$\text{CD}_3\text{NO}_2$	$\text{NC-CH}_3$ 2.25 (3, s), 2.37 (3, s), $-\text{CH}_3$ , 3.22 (12, s), $-\text{CH}_2$ 4.6-6.1 (12, m)
<i>anti</i> - $[\text{Co}(\text{C}_{14}\text{H}_{24}\text{N}_8\text{O}_2)(\text{CH}_3\text{CN})_2](\text{ClO}_4)_3$	$\text{CD}_3\text{NO}_2$	$\text{NC-CH}_3$ 2.32 (6, s), $-\text{CH}_3$ 3.22 (12, s), $-\text{CH}_2$ 4.6-6.1 (12, m)
$[\text{Ni}(\text{C}_{14}\text{H}_{24}\text{N}_8\text{O}_2)](\text{ClO}_4)_2$	$\text{CF}_3\text{COOD}$	$-\text{CH}_3$ 2.61 (12, s), $-\text{CH}_2$ 4.2-5.6 (12, m)

<sup>a</sup> Exchanged with  $\text{CD}_3\text{CN}$ . <sup>b</sup> Key: s = singlet; m = overlapping multiplets.

The products incorporate four formaldehyde residues into two  $-\text{CH}_2-\text{O}-\text{CH}_2-$  linkages with each end attached to one of the uncoordinated nitrogen atoms of the six-membered chelate rings. The formation of structural isomers having *syn* or *anti* conformations of the ether linkages with respect to the nominal plane of the macrocyclic ligand has been demonstrated (vide infra).

The chemical properties of the tricyclic ligand complexes are considerably different from their simple 14-membered macrocyclic precursors. The "simple" 14-membered macrocyclic ring complexes fragment in acidic media and readily deprotonate under mildly basic conditions, and the ligands readily undergo a variety of oxidation and reduction reactions. In contrast the tricyclic complexes are remarkably inert. For example, the Ni(II) complexes can be dissolved in concentrated sulfuric acid (one of the few solvents in which appreciable quantities of the compound can be dissolved), with insignificant ligand decomposition occurring even after several days. The Fe(II) complexes, like most Fe(II) complexes of  $\alpha$ -diimine ligands, are unreactive toward molecular oxygen.

Attempts to induce *syn-anti* isomerization of the imine linkages to VII by prolonged heating (days) of the compounds



in solution or by irradiation with ultraviolet light were unsuccessful.

The NMR and IR spectra of the new complexes, together with the analytical data, provided the necessary information for their structural interpretation. The IR spectra of all the tricyclic complexes are similar; no absorptions are present to indicate the presence of  $\text{NH}_2$ ,  $\text{NH}$ , or carbonyl groups. The  $\alpha$ -diimine functions give rise to weak absorptions in the vicinity of  $1550-1630\text{ cm}^{-1}$ ; these vary in position and intensity, depending upon the amount of  $d\pi(\text{metal})-p\pi(\alpha\text{-diimine})$  bond interaction. For example, the  $\alpha$ -diimine absorptions of the Fe(II) and Ni(II) complexes are so weak as to be virtually undetectable but are of moderate intensity in the Co(II) complexes. Similarly, large variations exist in the intensity of the  $\text{C}\equiv\text{N}$  absorption of the acetonitrile complexes. Those of the Fe(II) complex are very weak with a barely observable absorption at  $2300\text{ cm}^{-1}$  when thick Nujol mulls were used. The acetonitrile of the Co(III) complex has a moderately strong absorption at  $2350\text{ cm}^{-1}$ , while that of Co(II) occurs as three closely spaced peaks at  $2240$ ,  $2280$ , and  $2310\text{ cm}^{-1}$  and shifted only a few wavenumbers from the absorptions of free acetonitrile,  $2241\text{ cm}^{-1}$ ,<sup>16</sup> which was measured and superimposed on the same spectrum. The bis(isocyanide)

complex of Fe(II) had a very intense  $-\text{N}\equiv\text{C}$  absorption at  $2205\text{ cm}^{-1}$  compared to the free isocyanide of  $2169\text{ cm}^{-1}$ .<sup>17</sup>

The NMR spectra, Table VI, of the  $[\text{Co}(\text{C}_{14}\text{H}_{24}\text{N}_8\text{O}_2)(\text{CH}_3\text{CN})_2](\text{ClO}_4)_3$  and  $[\text{Fe}(\text{C}_{14}\text{H}_{24}\text{N}_8\text{O}_2)(\text{CH}_3\text{CN})_2](\text{ClO}_4)_2$  complexes provided indirect evidence for the existence of two isomers, VIb and VIa (hereafter designated *syn* and *anti*), of the macrocyclic ligand. The acetonitrile of the Co(III) complex and the methyl isocyanide of the Fe(II) complex are tightly bound and do not exchange with deuterioacetonitrile under the conditions used to obtain the  $^1\text{H}$  NMR spectra. The axially coordinated molecules of the complexes having the "syn" form of the ligand experience distinct chemical environments and give rise to separate resonances. The crude reaction product,  $[\text{Co}(\text{C}_{14}\text{H}_{24}\text{N}_8\text{O}_2)(\text{CH}_3\text{CN})_2](\text{ClO}_4)_3$ , obtained from the oxidation of the Co(II) complex in acetonitrile contains three peaks of approximate equal intensity in the acetonitrile region of the  $^1\text{H}$  NMR spectrum. Fractional recrystallization afforded two products, corresponding to the "syn" and "anti" isomers, with the *syn* isomer having  $\text{CH}_3\text{CN}$  resonances at  $\delta$  2.25 and 2.37 ppm; the equivalent  $\text{CH}_3\text{CN}$  groups of the *trans* isomer appear at 2.32 ppm. From the analysis of the crude reaction products, it appears that the ratio of the "syn" to "anti" form of the ligand when obtained from the formaldehyde condensation reaction of the five-coordinate Co(II) complex is about 2:1. The NMR spectrum of the bis(methyl isocyanide) complex of Fe(II) also contains three resonances attributable to the coordinated methyl isocyanide. The *anti* form appears to be the predominate isomer produced and gives rise to a single methyl isocyanide resonance at 3.15 ppm. Two peaks of equal but lesser intensity at 3.26 and 3.05 ppm are assigned to the unequal methyl isocyanides of the *syn* isomer. The positions of the remaining absorptions of the tricyclic ligand are virtually unchanged from those in the acetonitrile complexes (Table VI). In general, the two types of  $-\text{CH}_2-$  groups (those from the  $-\text{CH}_2-\text{O}-\text{CH}_2-$  and from the  $\text{N}-\text{CH}_2-\text{N}$  linkages) appear as unresolvable overlapping AB multiplet patterns between 4.5 and 6.0 ppm in all the complexes.

The resonances from the two types of the  $-\text{CH}_2-$  groups of the nickel complex were broad, possibly as a result of interconversion between boat and chair forms of the six-membered rings. Interaction of the oxygen atoms with the axial site of the metal is considered impossible in view of the results of the x-ray structural results.

The two  $\alpha$ -diimine chelate rings of the tricyclic ligand produce strong ligand fields. All of the tricyclic complexes are low spin. The Fe(II) and Co(III) complexes are six-coordinate and diamagnetic, the Ni(II) complex is square-planar and diamagnetic. The Co(II) and Cu(II) complexes have been isolated as five-coordinate species with water coordinated to one axial position, vide infra, and have magnetic moments of 2.0 and  $1.9\ \mu_B$ , respectively. The Co(II) complex of the stoichiometry  $[\text{Co}(\text{C}_{14}\text{H}_{24}\text{N}_8\text{O}_2)(\text{CH}_3\text{CN})_2](\text{ClO}_4)_2$  is believed to be six-coordinate, but with the acetonitrile bound

Table VII. Electronic Spectra of Tricyclic Complexes,  $[M(C_{14}H_{24}N_8O_2)L_2](ClO_4)_n$ 

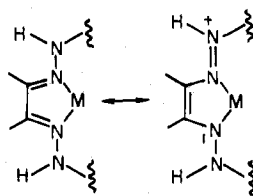
Compd	Solvent	Absorptions <sup>a</sup>
$[Fe(C_{14}H_{24}N_8O_2)(CH_3CN)_2](ClO_4)_2$	$CH_3CN$	551 ( $9.10 \times 10^3$ ), 515 ( $5.42 \times 10^3$ , sh), 309 ( $5.19 \times 10^3$ )
$[Fe(C_{14}H_{24}N_8O_2)(C_6H_5N)_2](ClO_4)_2$	$CH_3CN^b$	589 ( $8.03 \times 10^3$ ), 555 ( $6.10 \times 10^3$ ), 435 ( $9.87 \times 10^2$ ) 368 ( $3.68 \times 10^3$ ), 320 ( $5.80 \times 10^3$ )
$[Fe(C_{14}H_{24}N_8O_2)(NH_3)_2](ClO_4)_2$	$CH_3CN^b$	682 ( $1.08 \times 10^4$ ), 625 ( $5.85 \times 10^3$ , sh), 444 ( $4.08 \times 10^3$ ), 311 ( $4.85 \times 10^3$ )
$[Co(C_{14}H_{24}N_8O_2)(H_2O)](ClO_4)_2$	$H_2O$	510 ( $1.83 \times 10^3$ ), 288 ( $1.02 \times 10^4$ )
$[Co(C_{14}H_{24}N_8O_2)(CH_3CN)_2](ClO_4)_3$	$CH_3CN$	294 ( $1.44 \times 10^4$ ), 250 ( $8.67 \times 10^4$ )
$[Ni(C_{14}H_{24}N_8O_2)](ClO_4)_2$	$H_2SO_4$	370 ( $1.60 \times 10^3$ , sh), 282 ( $5.28 \times 10^3$ ), 233 ( $1.03 \times 10^4$ )
$[Cu(C_{14}H_{24}N_8O_2)(H_2O)](ClO_4)_2$	$CH_3CN^b$	523 ( $6.78 \times 10^2$ ), 319 ( $8.72 \times 10^3$ ), 248 ( $9.11 \times 10^3$ )

<sup>a</sup> Absorption in nm, extinction coefficient in parentheses. <sup>b</sup> Large excess of axial ligands were added.

only weakly to the axial coordination sites.

**Electronic Spectra of Tricyclic Complexes.** The data for the electronic spectra of the complexes are listed in Table VII. All the tricyclic complexes reported are very intensely colored. The electronic spectra are dominated by intense charge-transfer absorptions in the visible and ultraviolet portions of the spectra and obscure the d-d transitions that also occur in these regions. The charge-transfer bands of even the bis-(acetonitrile) complex of Co(III) tail into the visible region and precluded assignments of d-d transitions. The positions and intensities of these charge-transfer bands are sensitive to a multitude of factors, i.e., ligand field strength of the macrocyclic ligand, effects of the ligands on the redox potentials of the coordinated metal, the nature of the axial ligands, and the types of atoms and degree of unsaturation in the six-membered chelate rings. Solvents that interact with the  $\pi^*$  orbitals of the  $\alpha$ -diimine linkages are also known to influence these bands. Since the study of charge-transfer absorptions of complexes containing  $\alpha$ -diimine ligands has been largely relegated to those of Fe(II),<sup>18</sup> our comments will primarily be restricted to the complexes of Fe(II) also.

The electronic spectrum of  $[Fe(C_{14}H_{24}N_8O_2)(CH_3CN)_2](ClO_4)_2$  has intense absorption at 551 nm ( $\epsilon_{max}$   $9.0 \times 10^3$ ), approximately 100 nm lower than in the simple precursor macrocyclic complex,  $[Fe(C_{10}H_{20}N_8)(CH_3CN)_2]^{2+}$ , of I. This difference is attributed to the greater interaction between the lone electron pairs of the secondary nitrogen atoms and the  $\alpha$ -diimine functions in the latter complex. The flexibility associated with the six-membered chelate rings of I probably permits some flattening of the geometry about the secondary nitrogen atoms introducing a significant amount of  $sp^2$  character. This would enhance conjugation of the lone electron pair with the  $\alpha$ -diimine function, via resonance forms of the type depicted below. (This would also account for the



relative ease with which these nitrogen atoms are deprotonated.)

The configuration of the nitrogen atoms becomes rigidly fixed upon formation of the tricyclic structures, reinforcing the  $sp^3$  character of these atoms and preventing conjugation of the lone pairs with the  $\alpha$ -diimine functions.

The energy of the charge-transfer absorptions is dependent upon the axial ligands in a qualitatively predicted fashion. Basic ligands place increased electron density on the metal, raising the energy of the d orbitals, thus decreasing the gap between the metal and ligand  $\pi^*$  orbitals and give rise to red shifts. Strong  $\pi$ -acceptor ligands, i.e., cyanide and isocyanides, remove electron density from Fe(II) and increase the energy separation between the metal d orbitals and the  $\pi^*$ -acceptor

Table VIII. Interatomic Bond Distances (Å) for  $[Co(C_{14}H_{24}N_8O_2)(CH_3CN)_2](ClO_4)_3$ 

Co-N1	1.89 (1)	N3-C8	1.46 (2)
Co-N4	1.88 (1)	N4-C2	1.29 (2)
Co-N5	1.90 (1)	C2-C13	1.47 (2)
Co-N8	1.91 (1)	C2-C3	1.50 (2)
Co-N9	1.89 (1)	C3-N5	1.25 (2)
Co-N10	1.90 (1)	C3-C14	1.49 (2)
C11-O1	1.34 (2)	N5-N6	1.42 (2)
C11-O2	1.35 (2)	N6-C4	1.50 (2)
C11-O3	1.29 (2)	N6-C9	1.42 (2)
C11-O4	1.42 (2)	C4-N7	1.53 (2)
C12-O5	1.40 (1)	N7-C10	1.44 (2)
C12-O6	1.42 (2)	N7-N8	1.39 (2)
C12-O7	1.39 (1)	N8-C5	1.28 (2)
C12-O8	1.38 (2)	C5-C6	1.49 (2)
C13-O9	1.37 (2)	C5-C15	1.51 (2)
C13-O10	1.29 (2)	C6-C16	1.51 (2)
C13-O11	1.39 (2)	N9-C11	1.13 (2)
C13-O12	1.37 (2)	N10-C12	1.12 (2)
N1-N2	1.40 (1)	C11-C17	1.43 (2)
N1-C6	1.30 (2)	C12-C18	1.47 (2)
N2-C1	1.48 (2)	O13-C7	1.41 (2)
N2-C7	1.45 (2)	O13-C8	1.39 (2)
C1-N3	1.47 (2)	O14-C9	1.41 (2)
N3-N4	1.43 (1)	O14-C10	1.37 (2)

orbitals thus resulting in blue shifts.

**Description of the X-Ray Structures.**  $[Co(C_{14}H_{24}N_8O_2)(CH_3CN)_2](ClO_4)_3$ . The cation is composed of six-coordinate Co(III) of the form of the tricyclic ligand, VIb, with two acetonitrile molecules occupying the axial sites. The cation has approximate  $C_{2v}$  symmetry; the average of the chemically equivalent bond parameters will be used to describe the structure in view of the limited accuracy of the refinement.<sup>19</sup> The interatomic distances and angles for the structure are listed in Tables VIII and IX, respectively. A side view of the  $[Co(C_{14}H_{24}N_8O_2)(CH_3CN)_2]^{3+}$  cation, together with the atomic labeling scheme, is shown in Figure 1.

The parameters of the inner-coordination sphere are consistent with low-spin Co(III). The average Co-N<sub>4</sub> distance is 1.90 (1) Å, comparable to the Co-N distance, 1.89 Å, of a number of cobalt(III) dimethylglyoxime (DMG) complexes<sup>20</sup> and to another bis( $\alpha$ -diimine) macrocyclic Co(III) complex  $[Co([14]tetraeneN_4)(NH_3)_2]Br_3$  which has a Co-N planar distance of 1.90 (2) Å.<sup>21</sup> The average Co-N(CH<sub>3</sub>CN) bond length 1.89 (1) Å is virtually identical with the "in-plane" Co-N distance. This short bond length is indicative of strong CH<sub>3</sub>CN-Co<sup>III</sup> bonding and is supported by the very slow exchange rate of the axial CH<sub>3</sub>CN. No detectable exchange of coordinated CH<sub>3</sub>CN with CD<sub>3</sub>CN solvent was observed in a 2-week period. The Co-N distance is significantly shorter than the Co-N(NH<sub>3</sub>) distance, 1.972 (15) Å, observed in the  $[Co([14]tetraeneN_4)(NH_3)_2]^{3+}$  species.<sup>21</sup> This is attributable to the combined effects of hybridization differences about the nitrogen atom ( $sp$  hybridized for CH<sub>3</sub>CN vs.  $sp^3$  for NH<sub>3</sub>) and  $\pi$  bonding between the d $\pi$  orbitals of Co(III) and the orbitals of CH<sub>3</sub>CN. The short C $\equiv$ N distance, 1.12 (2) Å, is slightly shorter than that of free acetonitrile, 1.157 Å.<sup>24</sup> The Co-N

Table IX. Interatomic Angles (deg) for  $[\text{Co}(\text{C}_{14}\text{H}_{24}\text{N}_8\text{O}_2)(\text{CH}_3\text{CN})_2](\text{ClO}_4)_3$ 

N1-Co-N4	97.1 (4)	O10-C13-O11	103.2 (15)
N1-Co-N5	178.1 (4)	O10-C13-O12	114.5 (15)
N1-Co-N8	83.1 (5)	O11-C13-O12	100.2 (16)
N1-Co-N9	88.3 (4)	N2-N1-C6	120.8 (11)
N1-Co-N10	90.4 (4)	N1-N2-C1	109.1 (10)
N4-Co-N5	81.9 (4)	N1-N2-C7	112.4 (11)
N4-Co-N8	178.4 (4)	C1-N2-C7	111.2 (12)
N4-Co-N9	90.6 (4)	C1-N3-N4	109.2 (10)
N4-Co-N10	90.0 (4)	C1-N3-C8	109.4 (11)
N5-Co-N8	97.8 (5)	N4-N3-C8	110.9 (11)
N5-Co-N9	90.1 (4)	N3-N4-C2	119.7 (10)
N5-Co-N10	91.2 (4)	N6-N5-C3	120.6 (11)
N8-Co-N9	87.9 (4)	N5-N6-C4	110.4 (11)
N8-Co-N10	91.5 (4)	N5-N6-C9	112.1 (12)
N9-Co-N10	178.6 (4)	C4-N6-C9	111.7 (13)
O1-C11-O2	109.6 (15)	C4-N7-N8	111.6 (12)
O1-C11-O3	110.7 (14)	C4-N7-C10	107.5 (14)
O1-C11-O4	114.0 (10)	N8-N7-C10	109.3 (13)
O2-C11-O3	112.0 (19)	N7-N8-C5	122.1 (12)
O2-C11-O4	103.9 (14)	N2-C1-N3	113.7 (11)
O3-C11-O4	106.4 (15)	N4-C2-C3	112.5 (11)
O5-C12-O6	106.9 (9)	N4-C2-C13	126.6 (13)
O5-C12-O7	112.8 (8)	C3-C2-C13	120.9 (12)
O5-C12-O8	109.9 (9)	N5-C3-C2	112.7 (12)
O6-C12-O7	108.5 (10)	N5-C3-C14	126.1 (13)
O6-C12-O8	107.9 (12)	C2-C3-C14	121.2 (12)
O7-C12-O8	110.6 (11)	N6-C4-N7	110.5 (13)
O9-C13-O10	114.2 (12)	N8-C5-C6	115.7 (13)
O9-C13-O11	107.4 (13)	N8-C5-C15	124.5 (15)
O9-C13-O12	115.3 (12)	C6-C5-C15	119.8 (14)
N6-C9-O14	113.1 (13)	N1-C6-C5	111.8 (12)
N7-C10-O14	117.9 (17)	N1-C6-C16	125.2 (13)
N9-C11-C17	178.5 (16)	C5-C6-C16	123.0 (13)
C7-O13-C8	113.2 (13)	N2-C7-O13	112.2 (14)
C9-O14-C10	111.6 (14)	N3-C8-O13	113.1 (13)

Table X. Interatomic Distances (Å) and Angles (deg) for  $[\text{Cu}(\text{C}_{14}\text{H}_{24}\text{N}_8\text{O}_2)(\text{H}_2\text{O})](\text{ClO}_4)_2$ 

Cu-N1	1.944 (4)	N4-C5	1.462 (7)
Cu-N2	1.928 (4)	N4-N1 <sup>a</sup>	1.418 (5)
Cu-O5	2.262 (6)	O6-C4	1.419 (7)
N1-C1	1.285 (6)	O6-C5	1.421 (7)
C1-C2	1.500 (6)	C1-O1	1.356 (5)
C1-C6	1.487 (7)	C1-O2	1.280 (6)
C2-C7	1.477 (7)	C1-O3	1.355 (6)
C2-N2	1.283 (6)	C1-O4	1.267 (7)
N2-N3	1.419 (6)	O3-O5 <sup>b</sup>	3.094 (8)
N3-C3	1.487 (7)	O5-H13	0.94
N3-C4	1.472 (7)	O3-H13	2.43
N4-C3	1.477 (7)		
N1-Cu-N1'	164.6 (2)	N2-N3-C4	111.0 (4)
N1-Cu-N2	81.3 (2)	N2-N3-C3	109.1 (4)
N1-Cu-O5	97.7 (1)	C3-N3-C4	109.1 (4)
N2-Cu-N2'	165.8 (2)	C3-N4-N1'	108.4 (4)
N2-Cu-O5	97.1 (1)	C3-N4-C5	109.1 (4)
N2-Cu-O5	96.8 (2)	C5-N4-N1'	111.4 (4)
N4'-N1-Cu	120.9 (3)	N3-C3-N4	116.0 (5)
N4'-N1-C1	121.0 (4)	N3-C4-O6	112.7 (5)
Cu-N1-C1	115.7 (3)	N4-C5-O6	112.9 (5)
N1-C1-C6	124.7 (5)	C4-O6-C5	110.6 (5)
N1-C1-C2	113.8 (4)	O1-C1-O2	111.7 (5)
C2-C1-C6	121.5 (4)	O1-C1-O3	110.4 (4)
C1-C2-C7	120.8 (4)	O1-C1-O4	113.7 (2)
C1-C2-N2	113.1 (4)	O2-C1-O3	109.4 (6)
N2-C2-C7	126.1 (5)	O2-C1-O4	105.0 (7)
C2-N2-N3	120.3 (4)	O3-C1-O4	106.4 (6)
C2-N2-Cu	115.9 (3)	Cu-O5-H13	124
Cu-N2-N3	121.4 (3)	O5-H13-O3 <sup>b</sup>	128

<sup>a</sup> Primed atoms are transformed by  $-x, y, 1/2 - z$ . <sup>b</sup> O3 and O5 are involved in the hydrogen bonding.

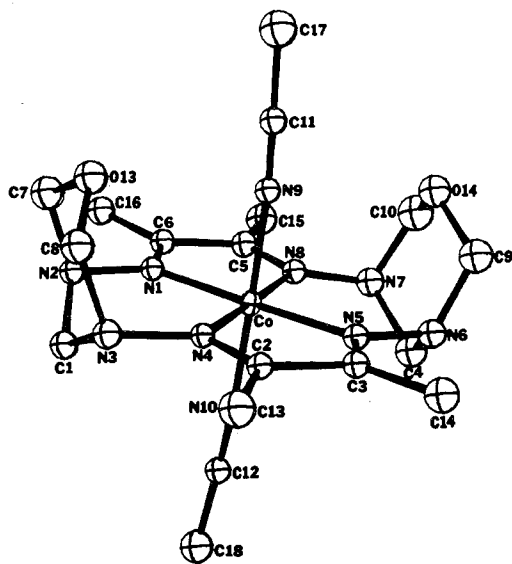


Figure 1. View of the  $[\text{Co}(\text{C}_{14}\text{H}_{24}\text{N}_8\text{O}_2)(\text{CH}_3\text{CN})_2]^{3+}$  cation together with the atom numbering scheme (ORTEP diagram, 20% probability ellipsoids).

and  $\text{C}\equiv\text{N}$  distances, as well as the higher  $\text{C}\equiv\text{N}$  stretching frequencies in the complex, lend greater credence to arguments based on hybridization than those based upon back-bonding schemes.

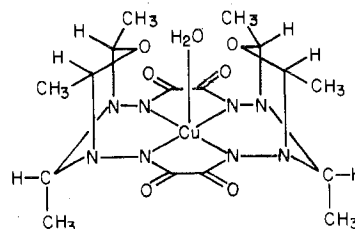
The average  $\text{C}=\text{N}$  bond length 1.28 (2) Å is only 0.01 Å longer than observed in a number of isolated imine ligand complexes and not judged to be significant. They are comparable to most other imine and  $\alpha$ -diimine containing ligands of other Fe(II) and Co(III) complexes.<sup>20,21</sup>

The two fused oxodiazia six-membered rings are "cis" with respect to the macrocyclic plane and each has a normal chair

conformation. The distance of the ether oxygen atoms from the axis defined by the axial sites is 2.869 Å; the distance of the oxygen atoms from the N atom of  $\text{CH}_3\text{CN}$  is 2.873 Å. This is slightly shorter than the sum of the normal van der Waals separation for these two atoms and indicates a slight amount of repulsive interaction between the two. If the repulsive interactions were severe, a boat conformation would be preferred by the oxodiazia rings.

$[\text{Cu}(\text{C}_{14}\text{H}_{24}\text{N}_8\text{O}_2)(\text{H}_2\text{O})](\text{ClO}_4)_2$ . The cation is composed of five-coordinate Cu(II) bound to the "cis" form of the tricyclic ligand and to a molecule of water. The molecule has crystallographic twofold symmetry with the  $\text{C}_2$  axis passing through the Cu atom and the oxygen of the water molecule. The final positional and thermal parameters for the nonhydrogen atoms are given in Table V. A side view of the cation, together with the atomic labeling scheme is shown in Figure 2.

The structure of the closely related copper compound, VIII,



VIII

obtained by the oxygenated condensation of oxalodihydrazide, acetaldehyde, and copper(II) has recently been reported.<sup>23</sup> The macrocycle of VIII formally contains four amide linkages and four negative charges. The major structural difference in the coordination sphere of the two types of copper(II) complexes is the placement of the molecule of water. In our structure, the water is opposite the side of the macrocyclic plane containing the ether linkages whereas in VIII the water molecule

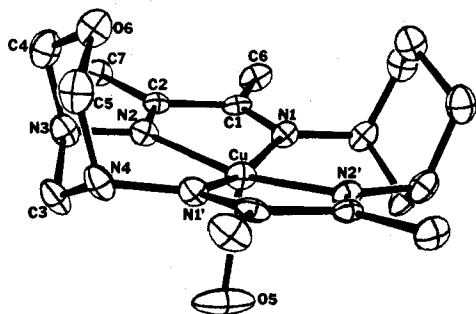
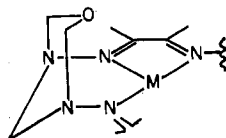


Figure 2. View of the  $[Cu(C_{14}H_{24}N_8O_2)(H_2O)]^{2+}$  cation together with the atom numbering scheme (ORTEP diagram, 20% probability ellipsoids).

Table XI. Comparison of the Average Bond Lengths (Å) of the Co(III) and Cu(II) Tricyclic Species



Compd	Co complex	Cu complex
C=N	1.279	1.284
C-C	1.496	1.500
C-CH <sub>3</sub>	1.497	1.484
N-N	1.409	1.418
C-N	1.469	1.474
O-C	1.394	1.420

is sandwiched between the ether oxygen atoms.

The average Cu-N(planar) distance in our structure, 1.936 (4) Å, is 0.04 Å longer than observed in the Co(III) complex and 0.08 Å longer than in the Cu(II) complex of VIII. The Cu-O(H<sub>2</sub>O) distance, 2.262 (6) Å, although long is not atypical of axial Cu(II)-O(H<sub>2</sub>O) distances. Despite the length and expected accompanying weakness of the Cu(II)-OH<sub>2</sub> bond, it has the effect of leading to a significant displacement, 0.25 Å, of the Cu atom from the least-squares plane defined by the N<sub>4</sub> donor atoms. Displacement resulting from the donor pairs being directly slightly out of the plane, as in other macrocyclic structures,<sup>24,25</sup> can be discounted because the displacement, 0.15 Å in VIII, is opposite in direction with respect to the oxodiazia rings but toward the axially coordinated water which has a long Cu-O(H<sub>2</sub>O) distance, 2.74 (1) Å.

The geometry of the polycyclic ligand of the Cu(II) and Co(III) complex is not significantly different. The average bond lengths of the two structures are compared in Table XI. The distance of the ether oxygen atom from the twofold axis is 2.656 Å, 0.21 Å closer than observed in the Co(III) structure, and is attributable to the absence of a ligand.

The water is symmetrically hydrogen bonded to the two ClO<sub>4</sub><sup>-</sup> anions related by a twofold rotation axis (Figure 3). Assuming a standard O-H distance of 0.958 Å for H<sub>2</sub>O, the hydrogen bonded O3-H13 distance is 2.41 Å and the O3-H13-O5 angle is 128°. Hydrogen bonding involving the ClO<sub>4</sub><sup>-</sup> anion is probably responsible for the ClO<sub>4</sub><sup>-</sup> positional parameters being better defined than in the Co(III) complex for which hydrogen bonding interactions are absent. Inspection of the thermal ellipsoids of the oxygen of the water molecule (Figure 3) clearly shows that motion of the oxygen atom is perpendicular to the hydrogen bond direction. Disorder in which the water molecule was unsymmetrically bound to the perchlorate anions would lead to apparent thermal motions along the direction of the hydrogen bond.

**Comparison with Related Structures.** Precession photographs of the cobalt(II) complex,  $[Cu(C_{14}H_{24}N_8O_2)(H_2O)](ClO_4)_2$ , indicated isomorphism with the Cu(II) complex.

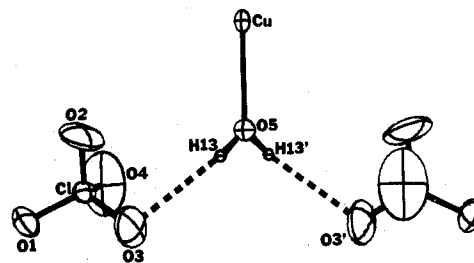


Figure 3. ORTEP plot illustrating the orientation of the coordinated water molecule with respect to the perchlorate anions.

The refined lattice parameters for the Co(II) are listed in Table I. Since the *b* cell axis is 0.291 Å longer in the Co(II) complex and since the molecules are constrained to lie along this axis (the crystallographic twofold axis), it may be speculated that the Co<sup>II</sup>-OH<sub>2</sub> bond is longer than in the Cu(II) complex. Axial ligation of low-spin Co(II) complexes is generally weak; Co<sup>II</sup>-O(H<sub>2</sub>O) distances of related complexes in the range 2.29<sup>21</sup> to 2.48 Å<sup>26</sup> have been observed.

### Conclusions

The results of the x-ray structural studies show that the ether oxygen atoms of the tricyclic ligand are too far removed from the central metal to interact significantly. These oxygen atoms are also far enough away from the axial site to allow small molecules such as acetonitrile and water to occupy these sites without serious steric interactions. More bulky axial ligands, e.g., quinuclidine, substituted phosphines, etc., might produce sufficient interaction to force the oxodiazia six-membered rings to assume a boat conformation.

It may only be fortuitous that the structures reported herein and those by Waters et al. have the *syn* arrangement of the oxodiazia six-membered rings. A possible explanation is the following. In the absence of interactions with axial ligands, as in four-coordinate square-planar complexes, the "cis" and "trans" tricyclic ligand isomers are expected to have approximately the same stability and to form in equal amounts. When the condensation reactions yielding the oxodiazia six-membered rings take place on metal complexes which are five-coordinate, such as many low-spin Co(II) and Cu(II) systems, the *syn* isomer will have the greater probability of forming. Steric interactions of the condensing formaldehyde units with the axial substituents, especially large bulky ligands, would inhibit condensation on the side containing the axial ligand. The observation of the "syn" isomer predominating with the Co(III) complexes and the Cu(II) complexes may thus be related to the five-coordinate nature of the precursors. In those cases where the oxodiazia six-membered rings are formed on six-coordinate precursors, such as low-spin Fe(II) and Co(III) complexes, the *trans* isomer is predicted to form in slight excess because both axial ligands can tip slightly to one side partially relieving the steric interaction.

**Acknowledgment.** This research was supported in part by the National Institutes of Health, Grant No. HL 14827.

**Registry No.**  $[Ni(C_{10}H_{20}N_8)](ClO_4)_2$ , 60086-90-0;  $[Fe(C_{10}H_{20}N_8)](ClO_4)_2$ , 65036-01-3;  $[Cu(C_{10}H_{20}N_8)Cl(H_2O)]ClO_4$ , 60119-39-3;  $[Co(C_{10}H_{20}N_8)](ClO_4)_2$ , 60086-91-1; CH<sub>2</sub>O, 50-00-0;  $[Fe(C_{14}H_{24}N_8O_2)(CH_3CN)_2](ClO_4)_2$ , 40471-72-5; *syn*- $[Fe(C_{14}H_{24}N_8O_2)(CNCH_3)_2](ClO_4)_2$ , 65036-03-5; *anti*- $[Fe(C_{14}H_{24}N_8O_2)(CNCH_3)_2](ClO_4)_2$ , 65084-51-7; *syn*- $[Co(C_{14}H_{24}N_8O_2)(CH_3CN)_2](ClO_4)_3$ , 65084-53-9; *anti*- $[Co(C_{14}H_{24}N_8O_2)(CH_3CN)_2](ClO_4)_3$ , 65084-55-1;  $[Ni(C_{14}H_{24}N_8O_2)](ClO_4)_2$ , 65036-04-6;  $[Fe(C_{14}H_{24}N_8O_2)(C_5H_5N)_2](ClO_4)_2$ , 65059-33-8;  $[Fe(C_{14}H_{24}N_8O_2)(NH_3)_2](ClO_4)_2$ , 65036-06-8;  $[Co(C_{14}H_{24}N_8O_2)(H_2O)](ClO_4)_2$ , 65027-62-5;  $[Co(C_{14}H_{24}N_8O_2)(CH_3CN)_2](ClO_4)_3$ , 65027-64-7;  $[Cu(C_{14}H_{24}N_8O_2)(H_2O)](ClO_4)_2$ , 65036-42-2;  $[Fe(C_{14}H_{24}N_8O_2)(NCS)_2]$ , 65027-65-8;  $[Co(C_{14}H_{24}N_8O_2)(CH_3CN)_2](ClO_4)_2$ , 65027-67-0.



**Supplementary Material Available:** A listing of hydrogen atom coordinates and the observed and calculated structure factor amplitudes is available (40 pages). Ordering information is given on any current masthead page.

## References and Notes

- Author to whom correspondence should be sent at the Department of Chemistry, Florida State University, Tallahassee, Florida 32306.
- J. P. Collman, R. R. Gagne, T. R. Halbert, J. C. Marchon, and C. A. Reed, *J. Am. Chem. Soc.*, **96**, 2629 (1974); J. P. Collman, R. R. Gagne, C. A. Reed, and W. T. Robinson, *Proc. Natl. Acad. Sci. U.S.A.*, **71**, 1326 (1974); J. Almog, J. E. Baldwin, R. L. Dyer, and M. Peters, *J. Am. Chem. Soc.*, **97**, 226 (1975); J. E. Baldwin and J. Huff, *ibid.*, **95**, 5757 (1973).
- J. Geibel, C. K. Chang, and T. G. Traylor, *J. Am. Chem. Soc.*, **97**, 5926 (1975), and references cited therein.
- D. G. Pillsbury and D. H. Busch, unpublished results.
- S.-M. Peng and V. L. Goedken, *J. Chem. Soc., Chem. Commun.*, 62 (1973); S.-M. Peng and V. L. Goedken, *Inorg. Chem.*, in press. The formation of noncyclic tetradentate ligands from the metal template condensation reactions of hydrazones with carbonyls has also been recently reported (C. M. Kerwin and G. A. Melson, *ibid.*, **11**, 726 (1972)).
- F. G. Riddell and P. Murray-Rust, *Chem. Commun.*, 1075 (1970).
- M. Suh and V. L. Goedken, to be submitted for publication. The macrobicyclic nitrogen cage recently reported by Sargeson et al. (I. I. Creaser, J. MacB. Harrowfield, A. J. Herlt, A. M. Sargeson, J. Springborg, R. J. Geue, and M. R. Snow, *J. Am. Chem. Soc.*, **99**, 3182 (1977)) probably proceeds through a similar intermediate.
- "International Tables for X-Ray Crystallography", Vol. I, 2nd ed, Kynoch Press, Birmingham, England, pp 89 and 101.
- Reference 8, p 150.
- The obtainment of the refined lattice constants and the data collection was facilitated by the automatic diffractometer control program of Lenhart.
- P. G. Lenhart, *J. Appl. Crystallogr.*, **8**, 568 (1975).
- W. Busing and H. A. Levy, *J. Chem. Phys.*, **26**, 563 (1957); P. W. R. Corfield, R. Doedens, and J. A. Ibers, *Inorg. Chem.*, **6**, 197 (1967).
- Computations were performed on an IBM 370 computer with the aid of the following programs: Zalkin's FORADP Fourier Program, Busing and Levy's ORFF function and error program, and Ibers's NUCLS least-squares program. Plots of the structures were drawn with the aid of C. K. Johnson's ORTEP.
- Neutral atom scattering factors were taken from D. T. Cromer and J. B. Mann, *Acta Crystallogr., Sect. A*, **24**, 321 (1968). Hydrogen atom scattering factors were taken from "International Tables for X-Ray Crystallography", Vol. III, Kynoch Press, Birmingham, England, 1962.
- D. T. Cromer, *Acta Crystallogr.*, **18**, 17 (1965).
- M. R. Churchill, *Inorg. Chem.*, **12**, 1213 (1973).
- E. L. Pace and L. J. Noe, *J. Chem. Phys.*, **49**, 5317 (1968).
- F. A. Cotton and F. Zingales, *J. Am. Chem. Soc.*, **83**, 351 (1961).
- P. Krumholz, *Struct. Bonding (Berlin)*, **9**, 129 (1971), and references cited therein.
- The number in parentheses following each distance denotes the mean of the estimated standard for the chemically equivalent bond distances.
- S. Brückner and L. Randaccio, *J. Chem. Soc. Dalton Trans.*, 1017 (1974), and references cited therein.
- M. D. Glick, W. G. Schmonsees, and J. F. Endicott, *J. Am. Chem. Soc.*, **96**, 5661 (1974).
- C. C. Costain, *J. Chem. Phys.*, **29**, 864 (1958); L. F. Thomas, E. I. Sherrard, and J. Sheridan, *Trans. Faraday Soc.*, **51**, 619 (1955).
- G. R. Clark, B. W. Skelton, and T. N. Waters, *J. Chem. Soc., Dalton Trans.*, 1528 (1976).
- M. C. Weiss, B. Bursten, S.-M. Peng, and V. L. Goedken, *J. Am. Chem. Soc.*, **98**, 8021 (1976).
- M. J. D'Aniello, Jr., M. T. Mocella, F. Wagner, E. K. Barefield, and I. C. Paul, *J. Am. Chem. Soc.*, **97**, 194 (1975).
- M. D. Glick, J. M. Kuszaj, and J. F. Endicott, *J. Am. Chem. Soc.*, **95**, 5098 (1973).

Contribution No. 5649 from the Arthur Amos Noyes Laboratory of Chemical Physics, California Institute of Technology, Pasadena, California 91125, and Contribution from the IBM Research Laboratories, San Jose, California 95193

## Further Studies of Metal-Metal Bonded Oligomers of Rhodium(I) Isocyanide Complexes. Crystal Structure Analysis of $[\text{Rh}_2(\text{CNPh})_8](\text{BPh}_4)_2$

KENT R. MANN, NATHAN S. LEWIS, ROGER M. WILLIAMS, HARRY B. GRAY,\* and J. G. GORDON II

Received August 15, 1977

The room-temperature electronic absorption spectra of  $[\text{Rh}(\text{CNR})_4]^+$  ( $\text{R} = \text{Ph}$ , *i*-Pr, cyclohexyl, *t*-Bu, vinyl) in solution do not follow Beer's law. This behavior has been attributed to oligomerization of  $[\text{Rh}(\text{CNR})_4]^+$  units to form species of the type  $[\text{Rh}_n(\text{CNR})_{4n}]^{n+}$ . Band maxima attributable to oligomers are as follows:  $\text{R} = \text{Ph}$ , 568 nm ( $n = 2$ ), 727 nm ( $n = 3$ ), in acetonitrile solution;  $\text{R} = t\text{-Bu}$ , 490 nm ( $n = 2$ ), 622 nm ( $n = 3$ ), in aqueous solution;  $\text{R} = i\text{-Pr}$ , 495 nm ( $n = 2$ ), 610 nm ( $n = 3$ ), in aqueous solution;  $\text{R} = \text{cyclohexyl}$ , 516 nm ( $n = 2$ ), in acetonitrile solution;  $\text{R} = \text{vinyl}$ , 555 nm ( $n = 2$ ), 715 nm ( $n = 3$ ), 962 nm ( $n = 4$ ), in aqueous solution. The molar extinction coefficients ( $\epsilon_n$ ) and formation constants  $K_{n-1}$  have been obtained for  $\text{R} = \text{Ph}$  in acetonitrile solution and  $\text{R} = t\text{-Bu}$  in aqueous solution. Parameter values are as follows: for  $\text{R} = \text{Ph}$ ,  $K_1 = 35 (15) \text{ M}^{-1}$ ,  $\epsilon_2 = 1.05 (20) \times 10^4$ ,  $\epsilon_3 K_2 = 1.83 (40) \times 10^5 \text{ M}^{-1}$ ; for  $\text{R} = t\text{-Bu}$ ,  $K_1 = 250 (125) \text{ M}^{-1}$ ,  $\epsilon_2 = 1.69 (34) \times 10^4$ . The x-ray crystal structure of  $[\text{Rh}(\text{CNPh})_4\text{BPh}_4]$  has been completed (final  $R = 0.057$ ). The compound crystallizes in the *Pbcn* space group ( $a = 23.80 (1)$ ,  $b = 19.23 (1)$ ,  $c = 19.08 (1) \text{ \AA}$ ) with four discrete cationic  $[\text{Rh}_2(\text{CNPh})_8]^{2+}$  units and eight  $\text{BPh}_4^-$  anions. The dimeric cation has idealized  $D_{4d}$  symmetry; the two  $[\text{Rh}(\text{CNPh})_4]^+$  units are bonded face to face so as to give a staggered configuration of ligands. The Rh-Rh distance is 3.193 Å. The electronic absorption spectra of  $D_{4d} [\text{Rh}_2(\text{CNR})_8]^{2+}$  and assumed  $D_{4h} [\text{Rh}_3(\text{CNR})_{12}]^{3+}$  complexes are interpreted in terms of the interactions expected between the occupied  $a_{1g}(d_{z^2})$  and unoccupied  $a_{2u}[p_x, \pi^*(\text{CNR})]$  monomer orbitals. The lowest band in each of the  $[\text{Rh}_2(\text{CNR})_8]^{2+}$  complexes is assigned to the allowed  $1b_2 \rightarrow 2a_1$  transition. In the spectra of  $[\text{Rh}_3(\text{CNR})_{12}]^{3+}$  complexes, the lowest band is attributed to  $2a_{1g} \rightarrow 2a_{2u}$ .

We are continuing systematic investigations of the ground- and excited-state physical and chemical properties of complexes in which metal( $d^8$ )-metal( $d^8$ ) interactions<sup>1-4</sup> are present. Systems that we have singled out for extensive study are based on planar rhodium(I) isocyanides.<sup>4-7</sup> In previous work we have established<sup>4</sup> that  $[\text{Rh}(\text{CNPh})_4]^+$  units oligomerize in acetonitrile solutions, yielding species such as  $[\text{Rh}_2(\text{CNPh})_8]^{2+}$  and  $[\text{Rh}_3(\text{CNPh})_{12}]^{3+}$ . The dimeric and trimeric complexes are characterized by intense low-lying electronic absorption bands, which fall at 568 and 727 nm, respectively. These electronic spectral characteristics coupled with infrared spectral results

led us to propose<sup>4</sup> that the structures of these oligomers feature face-to-face contact of  $[\text{Rh}(\text{CNPh})_4]^+$  units, with weak, direct Rh(I)-Rh(I) bonds. Purple crystalline samples of  $[\text{Rh}(\text{CNPh})_4\text{BPh}_4]$  have now been obtained, whose electronic spectra strongly suggest that dimeric  $[\text{Rh}_2(\text{CNPh})_8]^{2+}$  units are present. This paper reports the crystal structure analysis of  $[\text{Rh}(\text{CNPh})_4\text{BPh}_4]$ , as well as additional detailed spectral studies of the oligomerization reactions of several  $[\text{Rh}(\text{CNR})_4]^+$  complexes in solution.

## Experimental Section

The starting materials  $[\text{Rh}(\text{COD})\text{X}]_2$  ( $\text{X}^- = \text{Cl}^-, \text{Br}^-$ ) were prepared by the method of Chatt and Venanzi.<sup>8</sup> Phenyl, isopropyl, cyclohexyl,

\* To whom correspondence should be addressed at California Institute of Technology.